THE JOURNAL OF COMPARATIVE NEUROLOGY 332:499-513 (1993)

Spatial Distributions of Chemically Identified Intrinsic Neurons in Relation to Patch and Matrix Compartments of Rat Neostriatum

YOSHIYUKI KUBOTA AND YASUO KAWAGUCHI
Laboratory for Neural Systems, Frontier Research Program, The Institute of Physical and Chemical Research (RIKEN), Wako, Saitama 351-01, Japan

ABSTRACT

The spatial distributions and dendritic branching patterns of chemically identified subpopulations of striatal intrinsic neurons, defined by immunoreactivity for choline acetyltransferase (ChAT), neuropeptide Y or parvalbumin, were studied in relation to patch and matrix compartments of rat neostriatum. ChAT-immunoreactive cells and fibers showed an uneven pattern of distribution in the striatum. ChAT immunoreactivity was higher in the dorsolateral part and lower in the ventromedial part of the striatum. This regional gradient pattern is the inverse of the overall pattern of calbindin D_{28k} immunoreactivity. However, in small regions close to the lateral ventricle and globus pallidus, areas containing fewer ChAT-immunoreactive cells and fibers coincided with those containing low calbindin D_{28k} immunoreactivity. Neuropeptide Y immunoreactivity was uniform in the neostriatum. Certain neuropeptide Y cells (about 20%) were also immunoreactive for calbindin D_{28k}, indicating that at least a small population of calbindin D_{28k}-immunoreactive cells are medium aspiny cells. Parvalbumin immunoreactivity was not uniform in the striatum. A higher density of parvalbumin immunoreactivity was found in the neuropil in lateral and caudal parts than in the medial part. Small regions with weaker parvalbumin-immunoreactive neuropil partially corresponded to calbindin D_{28k} poor patches. Larger cells immunoreactive for parvalbumin were preferentially located in lateral and caudal parts of the striatum.

Cells immunoreactive for ChAT, neuropeptide Y or parvalbumin showed basically similar distribution patterns in relation to the patch and matrix compartments. Most stained cells were located in the matrix, but some were located at the borders of patches and a few were inside patches. Most primary dendrites of stained cells in the matrix or patches remained confined to these compartments, but cells on the borders invariably extended dendrites into both compartments. The striatal intrinsic neurons form chemically differentiated neuronal circuits within the matrix, and the patches and those whose dendrites cross the borders may contribute to associational interconnections between the two compartments, unlike the spiny projection neurons whose dendrites are confined to one or the other compartment.

Key words: acetylcholine, neuropeptide Y, parvalbumin, striatal mosaic, calbindin D_{28k}

The rat neostriatum is a heterogeneous structure with several different levels of anatomical organization. At one level it possesses topographically organized, region-specific connections with other parts of the brain. For instance, in the corticostriatal connection, sensorimotor cortex projects to the dorsolateral part while allocortex and mesocortex project to the ventromedial part of the striatum (MacGeorge and Faull, '89). Amygdalostriatal and ventral tegmental area-striatal projections terminate specifically in the ventromedial part of the striatum (Beckstead et al., '79; Kita and Kitai, '90). Striatal efferents projecting to the globus pallidus and substantia nigra are also topographically organized (Gerfen, '85b). At a second level, the striatum is divided into a mosaic of smaller compartments, the "patches and matrix." The patches were first identified as regions of high μ opiate receptor binding set in a matrix of lower receptor density (Herkenham and Pert, '81). Subsequent studies with a variety of techniques have revealed that the two compartments show further heterogeneity in their chemical anatomy and connectivity with other

Accepted February 23, 1993.

areas of the brain (Graybiel et al., '81; Gerfen, '85a; for reviews, see Graybiel, '90; Gerfen, '92). Pyramidal cells in different layers of the cerebral cortex project differentially to the patches or matrix. Striatal projection neurons located in the matrix compartment project to the GABAergic cells of the substantia nigra pars reticulata, while projection neurons in the patch compartment project to the ventral tier of the pars compacta and the pars reticulata. The recipient cells that form the ventral A9 dopaminergic group reciprocally project to the striatal patch compartment while other mesostriatal dopaminergic cell groups project to the striatal matrix compartment (Gerfen, '85b, '87a,b, '89; for a review, see '92). These distinct topographical and compartmental differences in connectional organization indicate that the neostriatum is a heterogeneously organized structure.

The neostriatum is composed of two main types of neurons: projection neurons and intrinsic neurons. The principal cell type is the medium spiny projection neuron and as much as 95% of the total striatal cell population belongs to this group (Graveland and DiFiglia, '85). The morphological features of this cell type are a medium-sized perikaryon and the possession of many dendritic spines (Dimova et al., '80; Chang et al., '82). Medium spiny projection neurons are located in both the patch and matrix compartments and their dendritic fields do not cross the boundaries of their compartments. There are few direct connections between the two compartments formed by the axons of projection neurons (Penny et al., '88; Kawaguchi et al., '89).

The remaining cells of the striatum, the aspiny intrinsic neurons, are characterized by cell bodies of variable size and aspiny or sparsely spiny dendrites (Dimova et al., '80; Chang et al., '82; Bolam et al., '84a). They show a number of distinct chemical differences. Recent immunohistochemical studies show that the largest aspiny intrinsic neurons are immunoreactive for choline acetyltransferase (ChAT) and that medium aspiny neurons are immunoreactive for somatostatin, neuropeptide Y, glutamate decarboxyrase (GAD), or parvalbumin (Bolam et al., '84b; Gerfen, '84, '85b; Chesselet and Graybiel, '86; Kita and Kitai, '88; Celio, '90). Somatostatin, neuropeptide Y and reduced nicotinamide adenine dinucleotide phosphate (NADPH) diaphorase have been colocalized in medium aspiny neurons as well as in nitric oxide synthase-positive cells (Vincent et al., '83; Dawson et al., '91). GAD and parvalbumin have been colocalized in medium to large aspiny intrinsic cells (Cowan et al., '90; Kita et al., '90). ChAT immunoreactivity is identified only in GAD-negative large neurons (Kita and Kitai, '88), or in NADPH-diaphorase and nitric oxide synthase-negative neurons (Dawson et al., '91). Parvalbumin cells and NADPH-diaphorase-positive neurons have been shown to be entirely separate subpopulations in the striatum (Kita et al., '90). These results indicate that striatal intrinsic neurons can be subdivided into at least three types, cholinergic large aspiny cells, neuropeptide Y-containing medium aspiny cells, and parvalbumin-positive, GABAergic medium to large aspiny cells.

The topographical distribution of striatal intrinsic neurons is not uniform (Phelps et al., '85; Cowan et al., '90; Kita et al., '90), but their exact distribution in relation to the patch and matrix compartments has not been completely elucidated, in particular, the extent to which their dendritic fields are restricted to individual compartments. The dendritic branching patterns of individual intrinsic cells in relation to the patch and matrix compartments could provide a morphological basis for cross-talk between the patch and matrix compartments, something that cannot be provided by the spiny projection neurons with their restricted dendritic fields. To investigate this issue, in the present study, the topographical distribution and dendritic branching patterns of three chemically identified types of intrinsic cells were investigated in relation to the patch and matrix compartments.

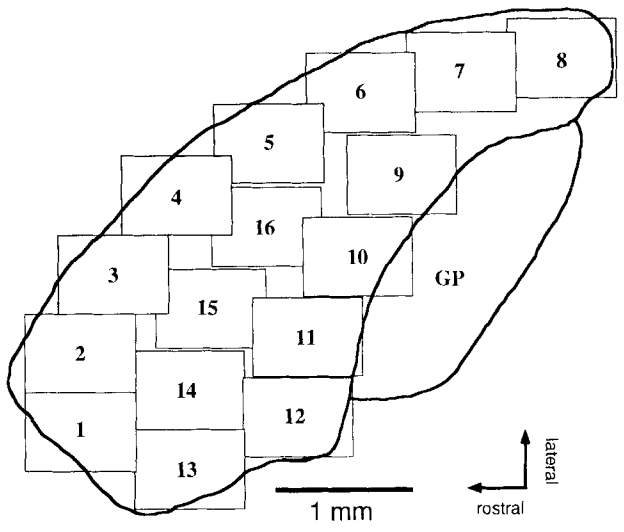

Fig. 1. Outline of the areas used for analysis on an oblique horizontal section of rat neostriatum. Each rectangle is 0.5 mm square. For the analysis of cell density, the number of the immunoreactive cells in each rectangle was counted. For the morphological analyses of individual immunoreactive cells, cells were chosen from particular rectangles and the cross-sectional somatic area and diameters were measured. GP, globus pallidus.

MATERIALS AND METHODS

Tissue preparation

Ten male Wistar rats (100–200 g) were used. The animals were anesthetized with an overdose of Nembutal and perfused through the heart with normal saline, followed by 300 ml of 4% paraformaldehyde containing 0.2% picric acid and 0.05% glutaraldehyde in 0.1 M sodium phosphate buffer (PB). The brains were removed and postfixed in the same fixative for 3 hours at 4°C. Oblique horizontal sections were cut on a vibratome along the line of the rhinal fissure (Kawaguchi et al., '89) or in the frontal or sagittal planes at 50 μm thickness. The tissue sections were put in glass tubes containing 15% sucrose in PB for 1 hour, frozen with liquid nitrogen and thawed at room temperature.

Immunocytochemical procedures

Throughout this investigation, calbindin D_{28k} immunoreactivity was used for the identification of the patch compartments since it is known that islands of weak calbindin D_{28k} immunoreactivity correspond to patches of high μ opiate receptor density and to weakly acetylcholinesterase-stained striosomes (for reviews, see Gerfen et al., '85a; Graybiel, '90). Two methods were used to identify the distribution of immunoreactive neurons and their dendritic branching

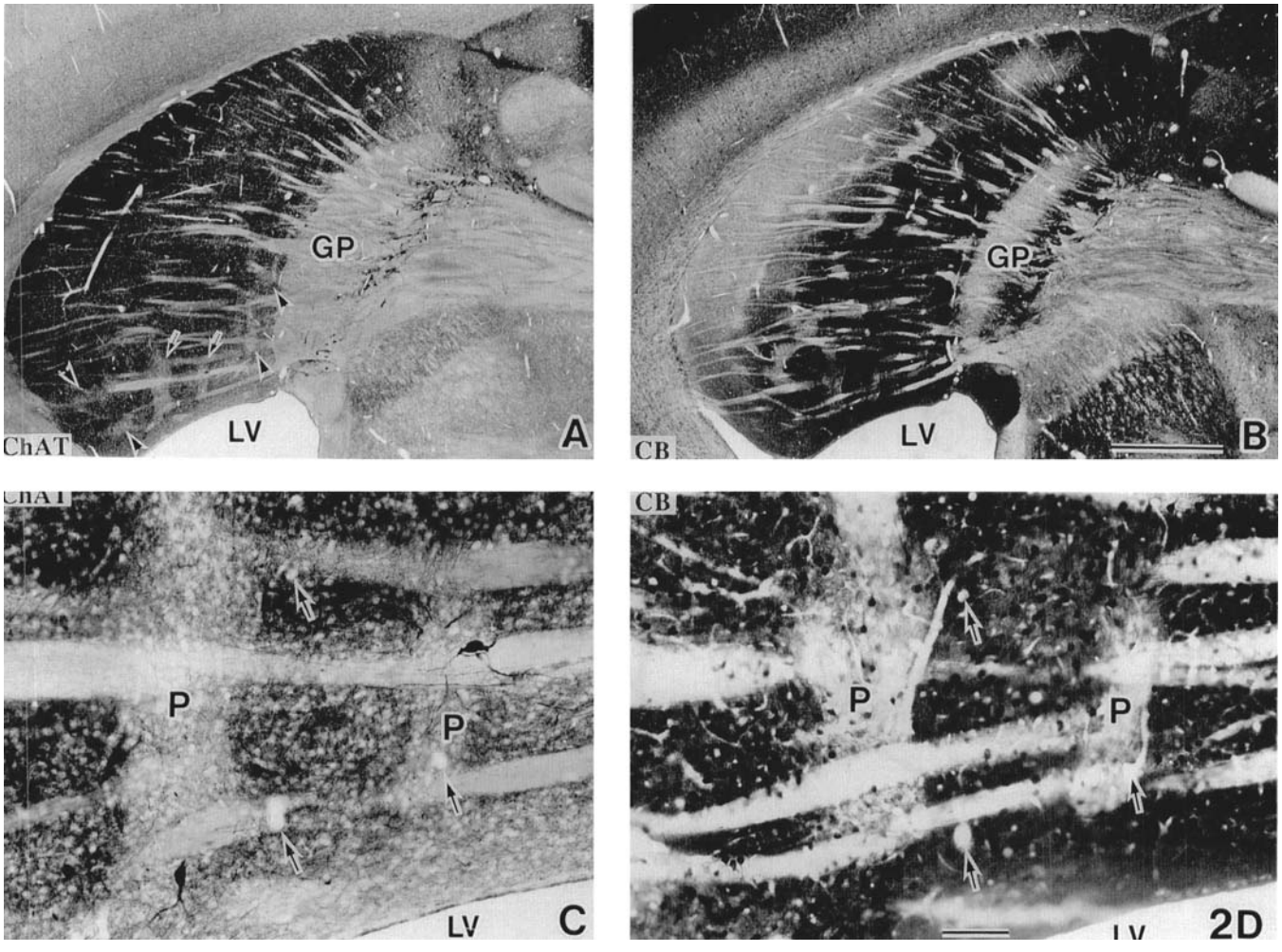

Fig. 2. **A:** ChAT immunoreactivity in an oblique horizontal section. Left and top are rostral and lateral, respectively. ChAT-poor regions can be seen (arrows and arrowheads). The rostrolateral part shows denser immunoreactivity, and regions close to the lateral ventricle (LV) and globus pallidus (GP) show weaker immunoreactivity. **B:** Calbindin D_{28k} immunoreactivity in the section adjacent to A. The rostrolateral region and the patch compartment show poor immunoreactivity. Note that ChAT immunoreactivity shows a pattern inverse to calbindin D_{28k} immunoreactivity. Denser ChAT staining area in the rostrolateral part corresponds to weaker calbindin-immunoreactive region. **C,D:** ChAT poor-immunoreactive neuropil regions (P) in the part of the striatum close to the lateral ventricle (C). The two poorly stained regions are those indicated by arrows in A. These poor regions are identical to calbindin D_{28k} poor patches (P) on the adjacent section (D). Arrows indicate capillaries as landmarks. CB, Calbindin D_{28k}. Scale bars = 1 mm for A and B, and 100 μm for C and D.

patterns in relation to the striatal patch and matrix compartments.

Mirror image method. Pairs of sections were immunostained for calbindin D_{28k} and for ChAT, neuropeptide Y, or parvalbumin. Sections were washed repeatedly in 0.05 M Tris-buffered saline (TBS). Alternate sections were then incubated overnight at room temperature either in rat monoclonal antibody against ChAT (0.1 mg/ml, Boehringer Mannheim) or mouse monoclonal antibody against calbindin D_{28k} (1:500, Sigma) in TBS containing 10% normal goat serum (NGS), 2% bovine serum albumin (BSA) and 0.5% Triton X-100 (TX). After washing 3 × 10 minutes with TBS, the sections were incubated in either biotinylated goat anti-rat IgG or biotinylated horse anti-mouse IgG (1:100, Vector Laboratories) for 60 minutes at room temperature. The sections were then washed 3 × 10 minutes in TBS and incubated in avidin:biotinylated horseradish peroxidase complex (ABC) complex in TBS *Elite* ABC, 1:100 each, Vector Laboratories) for 90 minutes at room temperature. After washing several times in TBS, the sections were rinsed with 0.05 M Tris HCl buffer (pH 7.6) (TB) for 5 minutes and immunoreactivity was visualized by the diaminobenzidine method. The sections were put in solution containing 3,3′-diaminobenzidine tetrahydrochloride (DAB, 0.05%) and H_2O_2 (0.01%) in TB. The reaction continued until the section turned deep brown and then was stopped by rinsing in TB. After washing in PB, the sections were treated with 1% osmic acid in PB for 1 hour. Subsequently, the sections were dehydrated with graded alcohols and then embedded between a slide and coverslip in Epon 812 (Fluka).

Further parallel series of sections were stained for neuropeptide Y or parvalbumin, using a rabbit antiserum against neuropeptide Y (1:500, Amersham) or a mouse monoclonal

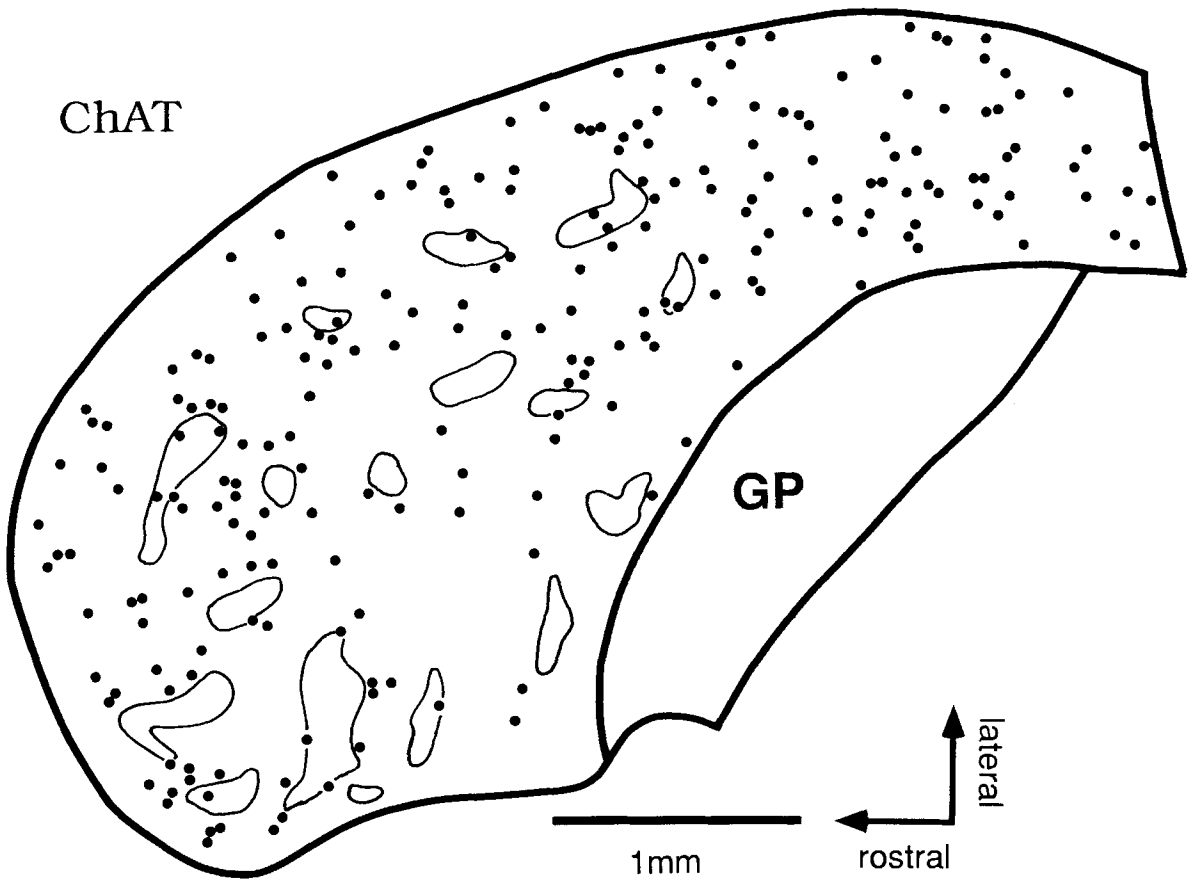

Fig. 3. Distribution pattern of ChAT-immunoreactive cells in the rat neostriatum in an oblique horizontal section. Patch compartments are outlined. The cells are mainly localized in the matrix compartment (outside the patches). Some cells are seen on or just outside the compartmental boundaries. Note that the cells are sparsely distributed in the region close to the lateral ventricle and globus pallidus. GP, globus pallidus.

TABLE 1. Cross-Sectional Somatic Areas and Diameters of Identified Cells in Rat Neostriatum

	Somatic area μm²	Somatic diameter (long axis), μm	Somatic diameter (short axis), μm	n
ChAT cells	285.1 ± 74.1[1] (157–439)	26.8 ± 6.6 (15.5–51.4)	16.0 ± 2.7 (10.1–24.3)	56
Neuropeptide Y cells	140.0 ± 33.4 (84–232)	18.2 ± 3.3 (12.2–25.0)	11.6 ± 2.0 (6.8–16.9)	44
Parvalbumin cells (total)	162.4 ± 54.2 (68–304)	18.0 ± 3.9 (10.1–27.7)	13.2 ± 2.5 (8.8–20.3)	136
Parvalbumin cells (rostral)[2]	129.4 ± 42.6* (68–259)	15.5 ± 2.7* (10.1–21.6)	12.0 ± 2.2* (8.8–18.9)	49
Parvalbumin cells (middle)[2]	158.3 ± 44.0 (79–265)	17.8 ± 3.3 (10.8–27)	13.3 ± 2.5 (8.8–18.2)	44
Parvalbumin cells (caudal)[2]	204.1 ± 48.3 (99–304)	21.0 ± 3.5 (14.2–27.7)	14.5 ± 2.3 (10.8–20.3)	43

[1]Data are mean ± SD. Range is in parenthesis. All values were measured on the oblique horizontal sections.
[2]The samples were picked up from areas 1 to 3, 11 to 15 in Figure 1 for the rostral part, areas 4 to 6, 9, 10, and 16 for the middle part, and 7, 8 for the caudal part.
*Significant differences between rostral and middle parts, middle and caudal parts, rostral and caudal parts of parvalbumin cells at $P \leq 0.05$.

antibody against parvalbumin (1:2,000, Sigma). For the secondary, biotinylated anti-rabbit serum or biotinylated anti-mouse serum (1:100, Vector Laboratories) was used and the sections treated in the same manner as above.

The dendrites and somata of immunoreactive cells were drawn using a 60× objective (N.A. 1.4) and a camera lucida. Camera lucida drawings of calbindin D_{28k} poor patches in the adjacent section were then superimposed, with the aid of capillaries and fiber bundles as landmarks. The immunoreactive cells per 50 square μm were counted in the light microscope with a 10× objective lens. The proportion of cross-sectional patch area to the cross-sectional area of the whole striatum was obtained from 5 different calbindin D_{28k}-immunostained, oblique horizontal sections, by computer-based image analysis (NEXUS QUBE). The somatic areas and the somatic diameters in the long and short axes of the immunoreactive cells were also analyzed by the computer-based image analysis. For statistical analysis in comparing parvalbumin-immunoreactive cells from different areas, the Mann-Whitney U test was used. An outline of the regions taken for analysis is illustrated in Figure 1.

Double indirect immunofluorescent method. Sections were double stained for calbindin D_{28k} and for neuropeptide Y, ChAT, or parvalbumin. Sections were washed several times in TBS and then incubated in the rabbit antiserum to neuropeptide Y and the mouse monoclonal antibody to calbindin D_{28k} in TBS containing 10% NGS, 2% BSA, and 0.5% TX overnight at room temperature. After washing 3 × 10 minutes in TBS, biotinylated goat anti-rabbit IgG (1:100, Vector Laboratories) and tetramethylrhodamine isothiocyanate (TRITC)-conjugated goat anti-mouse IgG

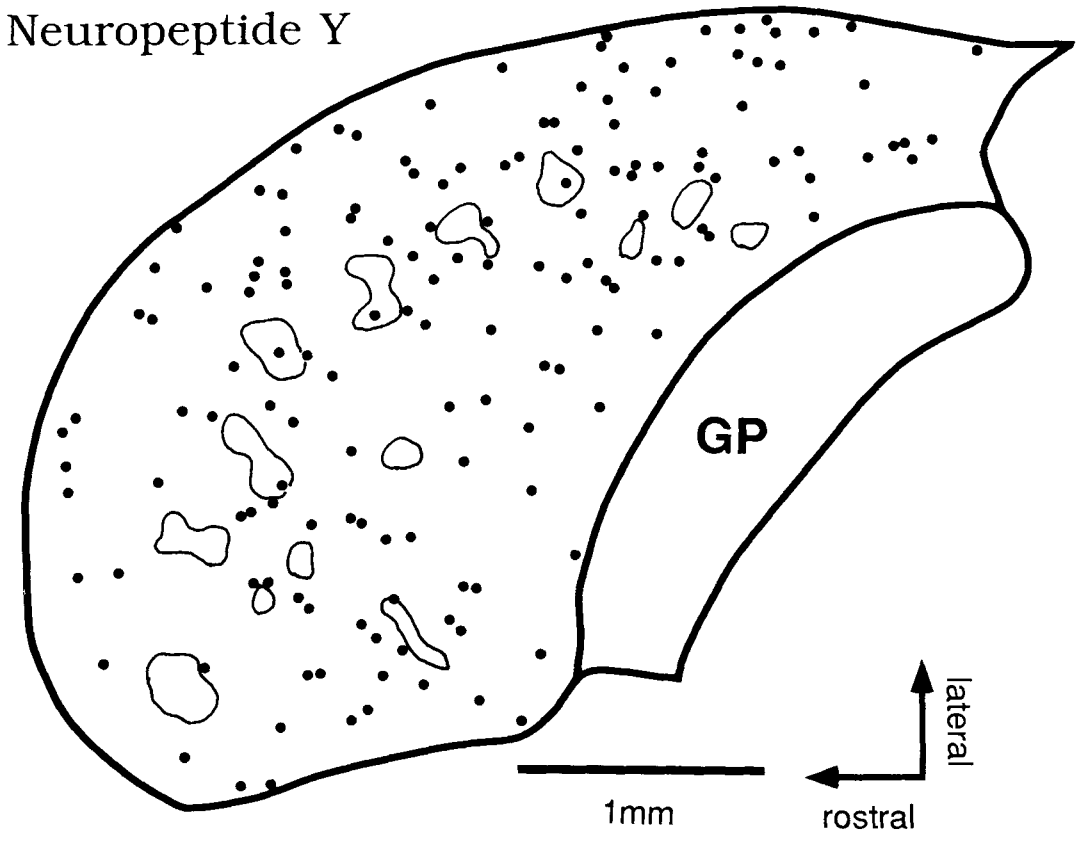

Fig. 4. Distribution pattern of neuropeptide Y-immunoreactive cells in the rat neostriatum in an oblique horizontal section. Patch compartments are outlined. The cells mainly localized in the matrix compartment (outside area of the patches). Some cells are seen on or just outside the compartmental boundaries. A few cells are seen in the patch compartments. GP, globus pallidus.

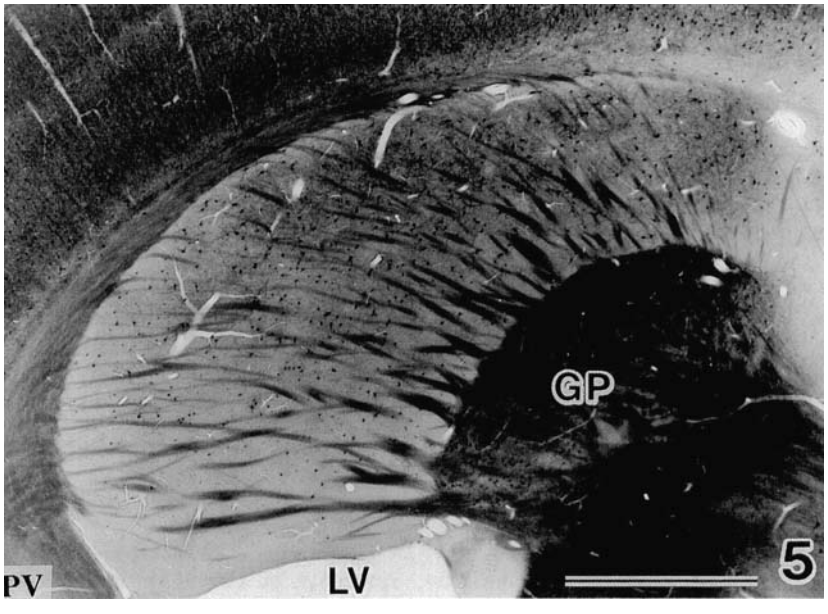

Fig. 5. Parvalbumin immunoreactivity in the neostriatum in an oblique horizontal section. A topographical immunoreactive neuropil gradient was seen, higher in lateral and caudal parts of the striatum and lower in medial part. Almost no staining area was seen close to the lateral ventricle. PV, parvalbumin; GP, globus pallidus; LV, lateral ventricle. Scale bar = 1 mm.

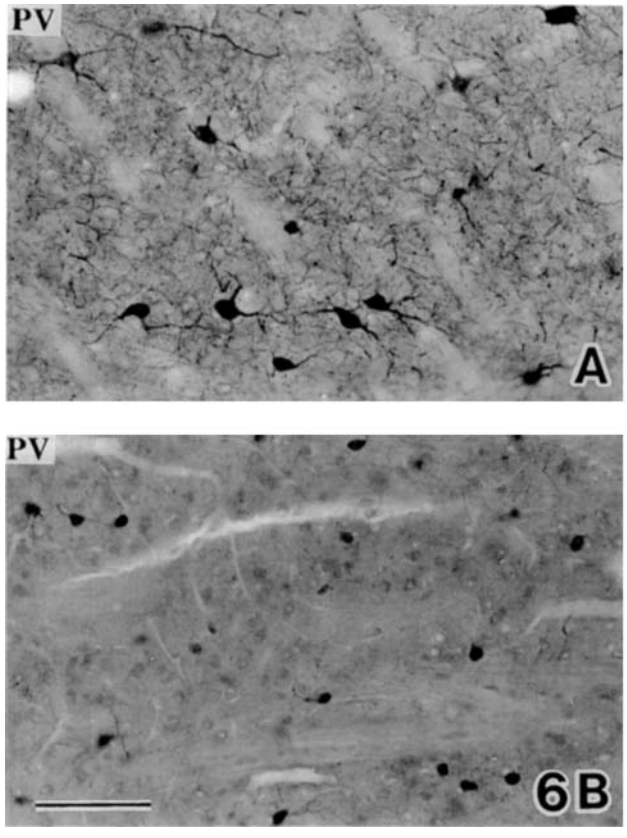

Fig. 6. Parvalbumin immunoreactivity in the neostriatum in an oblique horizontal section in the caudal part (**A**) and rostral part (**B**). Many larger cells and rich neuropil elements are seen in the caudal part and smaller cells and poor neuropil elements are seen in the rostral part. PV, parvalbumin. Scale bar = 100 μm.

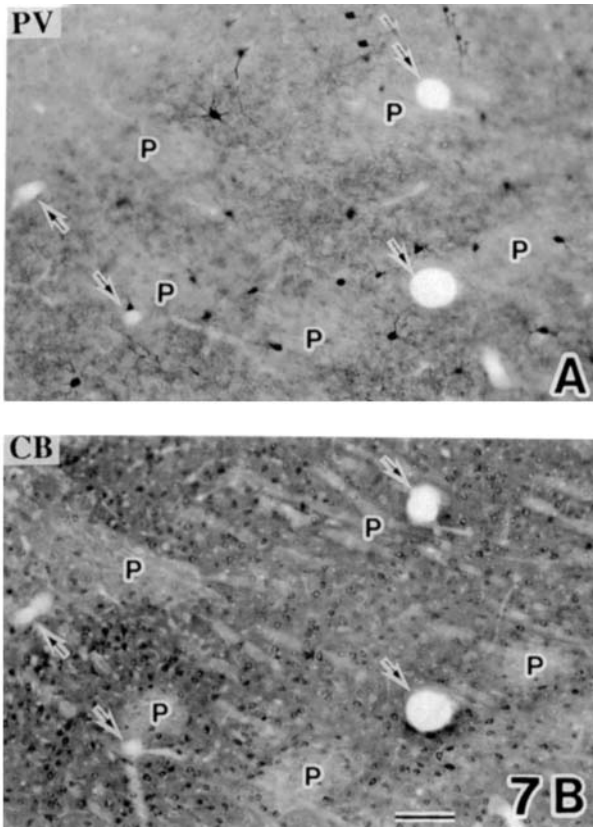

Fig. 7. Parvalbumin immunoreactivity in relation to the patch and matrix compartments. **A:** Parvalbumin immunoreactivity in the caudal part of the neostriatum in an oblique horizontal section. **B:** Calbindin D_{28k} immunoreactivity on the adjacent section. The parvalbumin poor regions (P) in A are confirmed to be identical to the calbindin D_{28k} poor patches. Arrows indicate capillaries as landmarks. CB, calbindin D_{28k}; PV, parvalbumin; P, patch compartments. Scale bar = 100 μm.

(1:100, Chemicon) in TBS were used as the secondary antibodies for 60 minutes at room temperature. The sections were then washed 3 × 10 minutes in TBS and incubated in streptavidin conjugated 7-amino-4-methylcoumarin-3-acetic acid (AMCA, 1:100, Vector Laboratories) in TBS for 90 minutes at room temperature. After washing 3 × 10 minutes in TBS, the sections were mounted on gelatin-coated glass slides in 50% glycerin in TBS. Then the sections were observed and photographed with the fluorescence microscope (Nikon Microphot-FXA) fitted with a dichroic mirror system G for TRITC or V for AMCA. Cell distribution patterns in relation to the patch and matrix compartments were analyzed by fluorescence microscopy and photographed. Subsequently, after washing several times in TBS, the sections were reincubated in ABC complex (ABC, Vector Laboratories) for 90 minutes at room temperature followed by the DAB reaction. Then sections were dehydrated in graded alcohols, osmicated and embedded between a slide and coverslip in Epon 812 (Fluka). The dendrites and somata were drawn with the aid of a 60× objective and camera lucida. The fluorescence photomicrographs previously taken to show calbindin D_{28k} poor immunoreactive patches were then superimposed on the camera lucida drawings of the cells, with capillaries and fiber bundles as landmarks.

Further parallel series of sections were stained for calbindin D_{28k} and ChAT or parvalbumin immunoreactivity, by rabbit antiserum against calbindin D_{28k} (from P.C. Emson, Hendry et al., '89) and the same rat monoclonal antibody against ChAT (1 mg/1 ml, Boehringer Mannheim) as above or a mouse monoclonal antibody against parvalbumin (1:2,000, Sigma). For parvalbumin and calbindin D_{28k} double immunohistochemistry, 10% normal horse serum was used instead of normal goat serum in the incubation buffer. For the secondary antiserum, biotinylated anti-rat IgG or mouse IgG (1:100, Vector Laboratories) and FITC-conjugated goat anti-rabbit IgG (1:100, Vector Laboratories) were used, following the same protocol as for calbindin D_{28k} and neuropeptide Y immunoreaction. Streptavidin-conjugated Texas red (1:100, Amersham) was used for the final incubation. G or B2 dichroic mirror illumination was used in the fluorescence microscope for visualizing Texas red or FITC, respectively.

Cross-reactivity of the secondary antibodies. The cross-reactivity of the secondary antibodies was checked by incubating sections first in a single primary antibody followed by a secondary antibody appropriate for a different primary. For instance, sections incubated with rabbit anti-neuropeptide Y were incubated in TRITC-conjugated goat

anti-mouse IgG. All six possible combinations were checked and no specific staining was identified.

RESULTS

Calbindin D_{28k}-immunoreactive structures

Calbindin D_{28k} immunoreactivity was not distributed evenly in the rat neostriatum. Weak immunoreactivity overall was observed in the dorsolateral part of the striatum. In the rest of the striatum, the matrix compartment could be identified containing dense calbindin D_{28k}-immunoreactive fibers and positive cells and the patch compartment could be identified as a series of regions of weak immunoreactivity (Fig. 2B). Calbindin D_{28k} weak patches formed 8.6% of the area of the striatum and this was consistent with a previous report (Johnston et al., '90). Occasional strongly calbindin D_{28k}-positive cells were identified in the calbindin D_{28k} poor dorsolateral striatum and in certain patch compartments.

The distributions of immunoreactive neuropil and cells

ChAT-immunoreactive structures. ChAT immunoreactivity in the striatum consisted of a dense fiber plexus and large stained cells. The density of immunoreactive fibers was high in dorsolateral and low in ventromedial parts of the neostriatum. In particular, a region close to the external capsule showed higher immunoreactivity and a region close to the lateral ventricle and globus pallidus showed lower immunoreactivity than elsewhere (Fig. 2A). This pattern is the reverse of the pattern of calbindin D_{28k} staining (Fig. 2B). In the region close to the lateral ventricle and globus pallidus, small regions showing a lower density of ChAT-immunoreactive neuropil could be identified. (Fig. 2A,C). These ChAT poor regions corresponded to calbindin D_{28k} poor patch compartments seen in the adjacent sections (Fig. 2C,D). The ChAT poor regions were mainly due to a low density of immunoreactive axons.

ChAT-immunoreactive cells showed an uneven distribution pattern (Fig. 3). The dorsolateral part of the striatum contained a larger number of ChAT-immunoreactive cells than the ventromedial part. Thus, in zones 1–7 (Fig. 1) there were 18.9 ± 5.26 cells per 0.5 square mm (n = 27), while zones 9–12 contained 8.0 ± 3.5 cells per 0.5 square mm (n = 16). In intermediate regions corresponding to zones 13–16, there were 12.1 ± 4.48 cells per 0.5 square mm (n = 12). The tail of the striatum (zone 8) contained 14.8 ± 4.03 cells per 0.5 square mm (n = 12). The ChAT-immunoreactive cells had large cell somata (Table 1) with two to six primary dendrites lacking dendritic spines. The cell bodies were polygonal or fusiform in shape.

Neuropeptide Y-immunoreactive structures. Neuropeptide Y-immunoreactive neuropil showed a low density overall and was distributed more evenly than the plexus of ChAT-immunoreactive fibers. Neuropeptide Y-immunoreactive fibers were seen in both patch and matrix compartments. Neuropeptide Y-immunoreactive neurons were also identified uniformly throughout the striatum (15.8 ± 5.03 cells per 0.5 square mm, n = 36) (Fig. 4). The cell bodies were of medium size (Table 1) and had polygonal or fusiform shapes. They had two to five primary dendrites that lacked dendritic spines.

Parvalbumin-immunoreactive structures. Parvalbumin-immunoreactive neuropil showed a topographical gradient of density with higher levels in the lateral and caudal part and lower levels in the medial part of the rostral striatum and in a band along the globus pallidus (Figs. 5, 6). A region in which staining was virtually absent was identified close to the lateral ventricle (Fig. 5).

Small regions showing weak immunoreactivity could also be detected within the region of higher density. These small parvalbumin poor regions were due to a low density of both stained axons and dendrites. When these regions were compared with the calbindin D_{28k} poor-immunoreactive patches in adjacent sections a number were found to be coextensive with the patches (Fig. 7). However, other small regions filled with parvalbumin-immunoreactive processes also corresponded to patches in certain regions.

The parvalbumin cells distributed evenly in most zones of the striatum (29.7 cells ± 8.87 per 0.5 square mm, n = 46), but larger cells were located in the lateral and caudal parts of the striatum (Table 1, Figs. 6, 8) and a band about 500 μm along the lateral ventricle and about 150 μm wide along the globus pallidus showed fewer parvalbumin-immunoreactive cells (16.4 cells ± 6.4 per 0.5 square mm, n = 7) (Fig. 8). Cell sizes varied from medium to large (Table 1). The somata of immunoreactive cells were polygonal, fusiform or round and three to ten aspiny primary dendrites radiated in all directions. The dendrites often curved and meandered, while branching profusely. Larger cells had more dendrites. Sometimes, single or clustered parvalbumin-immunoreactive somata were confined to patches (Fig. 8). Others were found in the matrix or overlapped both compartments.

Immunoreactive cells in relation to the patch and matrix compartment

The majority of immunoreactive cells were well stained and showed staining of primary, secondary, and tertiary dendrites. In many cases, however, because of the relative thinness of the sections, the more peripheral dendrites passed out of the plane of section; in others, they were less completely stained than more proximal dendrites. Hence, the relationships of cells to patches and matrix is primarily based on the distribution of the major dendritic branches. In general, axons were not stained much beyond their initial segments.

Cholinergic cells. The ChAT-immunoreactive cells were principally located within the matrix compartment (211 out of 239 cells, 88.3%) (Fig. 3). The dendrites usually remained within the matrix, but a few branches occasionally crossed into the patch compartment. Certain cells located within 20 μm of the border of a patch tended to extend their dendrites along this boundary (26 out of 239 cells, 10.9%) (Figs. 3, 9). Among this group of cells, a number of dendrites emerging from the patch side extended into the patch compartment and a number emerging on the matrix side extended into matrix compartment (Fig. 9). Cells were rarely seen at the center of a patch compartment (2 out of 239 cells, 0.8%) (Figs. 3, 9, 10). The primary dendrites of these few cells remained within the patch compartment (Fig. 9). Unfortunately, the most peripheral portions of dendrites immunoreactive for ChAT passed out of the plane of section. Some other stained dendrites, of which the cell soma was not identified on the section, were observed to cross the borders.

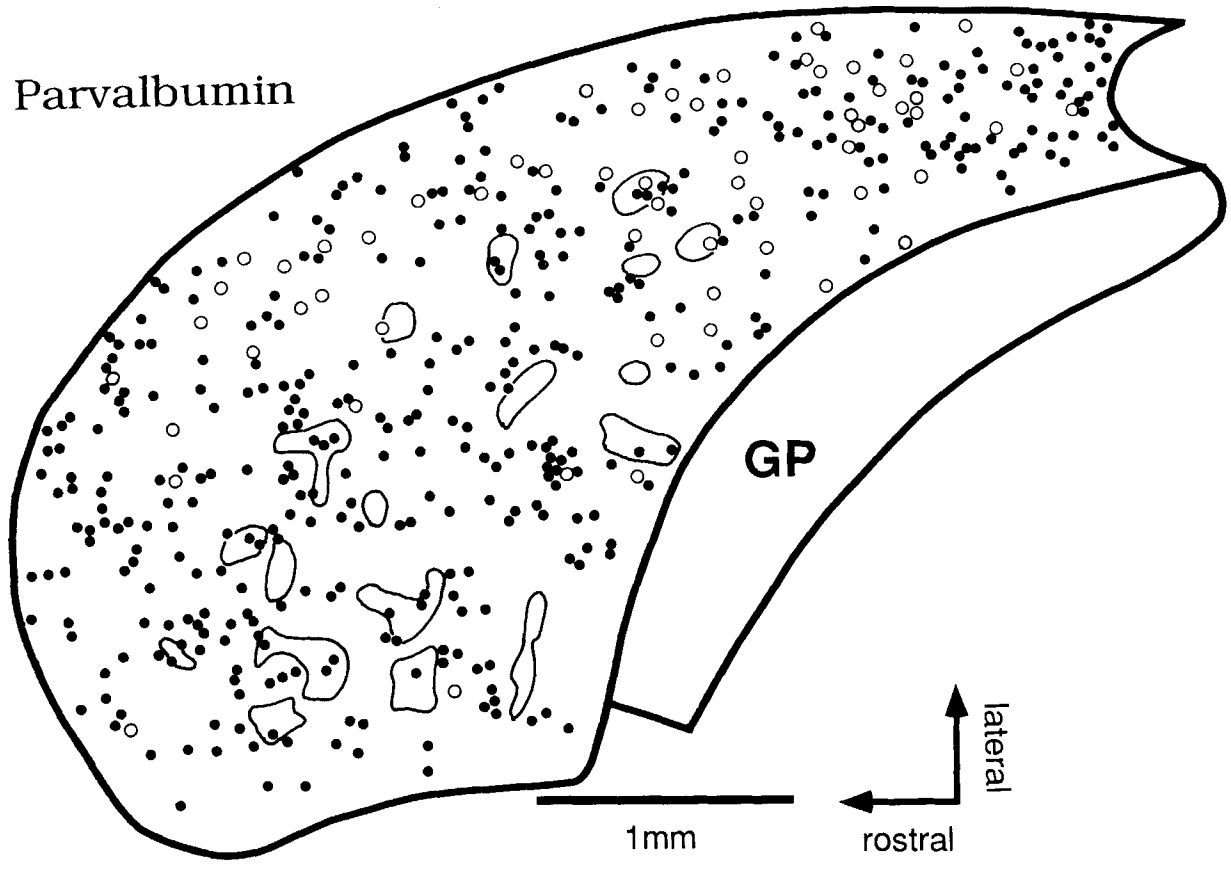

Fig. 8. Distribution pattern of parvalbumin-immunoreactive cells in an oblique horizontal section. Patch compartments are outlined. Open circles indicate larger cells (diameter in long axis ≥ 20 μm), and black circles indicate medium cells (diameter in long axis < 20 μm). The cells are mainly localized in the matrix compartment (outside the patches). Some cells are seen on the compartmental boundaries and in the patches. Note that the larger cells tend to distribute in the lateral and caudal part of the striatum. GP, globus pallidus.

Neuropeptide Y-immunoreactive cells. Most neuropeptide Y-immunoreactive neurons were located in the matrix compartment (214 out of 257 cells; 83.3%) (Fig. 4). Their dendrites tended to remain within the matrix compartment (Fig. 11). Cells located within 20 μm of the border between compartments usually extended dendrites into both compartments (37 out of 257 cells; 14.4%) (Fig. 11). A few cells were identified in the patch compartment (6 out of 257 cells; 2.3%) (Figs. 4, 12). The primary dendrites remained within the patch compartment, but branches arising from them crossed into the matrix compartment (Fig. 11). Other dendrites, of which the cell soma was not identified on the section, crossed the border between compartments.

Parvalbumin-immunoreactive cells. Most of the immunoreactive cells were located in the matrix compartment (386 out of 433 cells; 89.1%) (Fig. 8). The dendrites of many cells remained within the matrix compartment and certain dendrites arising from cells located in the matrix did not cross the compartmental boundary (Figs. 13, 14). Most cells located on the boundaries of the patch compartments (30 out of 433 cells; 6.9%) (Fig. 8), however, did extend dendrites into both compartments (Fig. 14). A small number of cells was identified in the patch compartments (17 out of 433 cells; 3.9%) (Figs. 8, 13, 14). The primary dendrites of these remained within the patch, but their distal parts or their branches crossed into the matrix compartment (Figs. 13, 14). A few parvalbumin-immunoreactive neurons were seen clustered in the same patch. Their dendrites covered a large part of the patch compartment (Fig. 14). The immunoreactive parvalbumin neurons in this study showed more complete dendritic field than other immunoreactive cells.

Coexistence of neuropeptide Y and calbindin D_{28k}

Certain neuropeptide Y-immunoreactive neurons were shown to possess calbindin D_{28k} immunoreactivity (92 out of 467 cells; 19.7%) by the double immunofluorescence method (Fig. 15). In the patch compartment, 21 out of 87 neuropeptide Y-immunoreactive cells (24.1%) showed colocalized calbindin D_{28k} immunoreactivity (Fig. 15A,B). In the matrix compartment, 24 out of 259 neuropeptide Y-immunoreactive cells (9.3%) showed colocalized calbindin D_{28k} immunoreactivity. In the dorsolateral part of the striatum, where calbindin D_{28k} immunoreactivity was weak, 47 out of 121 neuropeptide Y-immunoreactive cells (38.8%) showed colocalized calbindin D_{28k} immunoreactivity (Fig. 15C,D). The double immunoreactive cells showed particularly strong calbindin D_{28k} immunoreactivity and therefore they probably corresponded to the strong calbindin D_{28k}-immunoreactive cells occasionally found in calbindin D_{28k} poor regions.

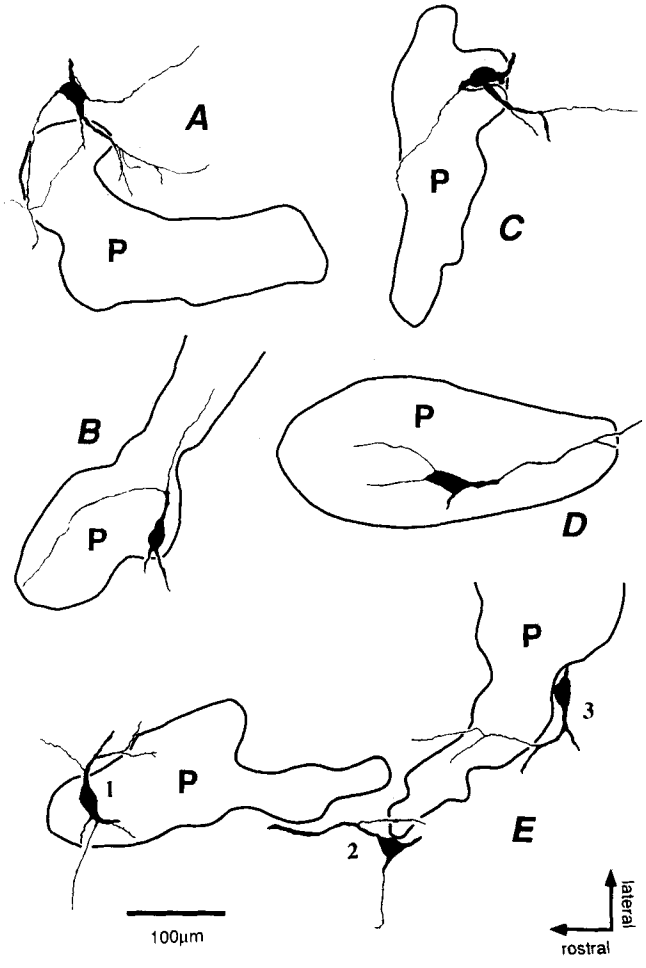

Fig. 9. **A–E:** Reconstruction of 7 ChAT-immunoreactive cells showing the relationship of dendritic branching patterns to the patch (P) and matrix (external to P) compartment in oblique horizontal section. Cells in C and cell 3 in E are the same cells as in Figure 2C. Cells are located on the boundaries (A–C, E). Some dendrites respect the compartmental boundary, but dendrites originating from them enter the patch (cells in A and E). The dendrites on the patch side elongate into the patch compartment and some of the distal part enter the matrix. The dendrites on the matrix side elongate into the matrix compartment (cells in A, B, C and 1 and 3 in E). The cell in the patch compartment extends the dendrites in the patch, but the branch elongates into the matrix compartment (D).

DISCUSSION

Immunoreactive dendritic branching pattern in relation to the striatal patch and matrix compartments

The present study showed the dendritic arborization patterns of three chemically distinct forms of intrinsic neurons in relation to the patch and matrix compartments of the rat striatum. Ninety percent of these striatal intrinsic cells are localized to the matrix compartment and this proportion is about the same as that of the area of matrix relative to that of the whole striatum. This suggests that striatal intrinsic neurons are distributed without preference for a particular striatal compartment. The dendrites of the majority of these intrinsic cells are located within the matrix. This suggests that they form components of neuronal circuits mainly within the matrix compartment. About 10% of the intrinsic cells, however, are located in the region within 20 μm of the borders between compartments, and these usually extend dendrites into both compartments. A small number of the intrinsic cells are also located in the patch compartments proper. Their primary dendrites extended mainly within the patch compartments, but branches arising from them also tended to cross the compartmental boundary into the matrix. The crossing of compartmental borders by the dendrites of many intrinsic cells situated close to or within the patches suggests that these cells may receive terminations of afferents ending in both compartments and serve as anatomical links between the two compartments. Parvalbumin-immunoreactive cells are found more frequently in the patch compartments than the other two chemically distinct types of intrinsic cells (3.9% of the total parvalbumin-immunoreactive cells). A few neuropeptide Y-immunoreactive cells are sometimes found in the patch compartment (2.3% of the total neuropeptide Y-immunoreactive cells). ChAT-immunoreactive cells are rarely located in the patches (0.8% of the total ChAT immunoreactive cells).

Previous studies (Penny et al., '88; Kawaguchi et al., '89) indicated that the common medium spiny cells of the

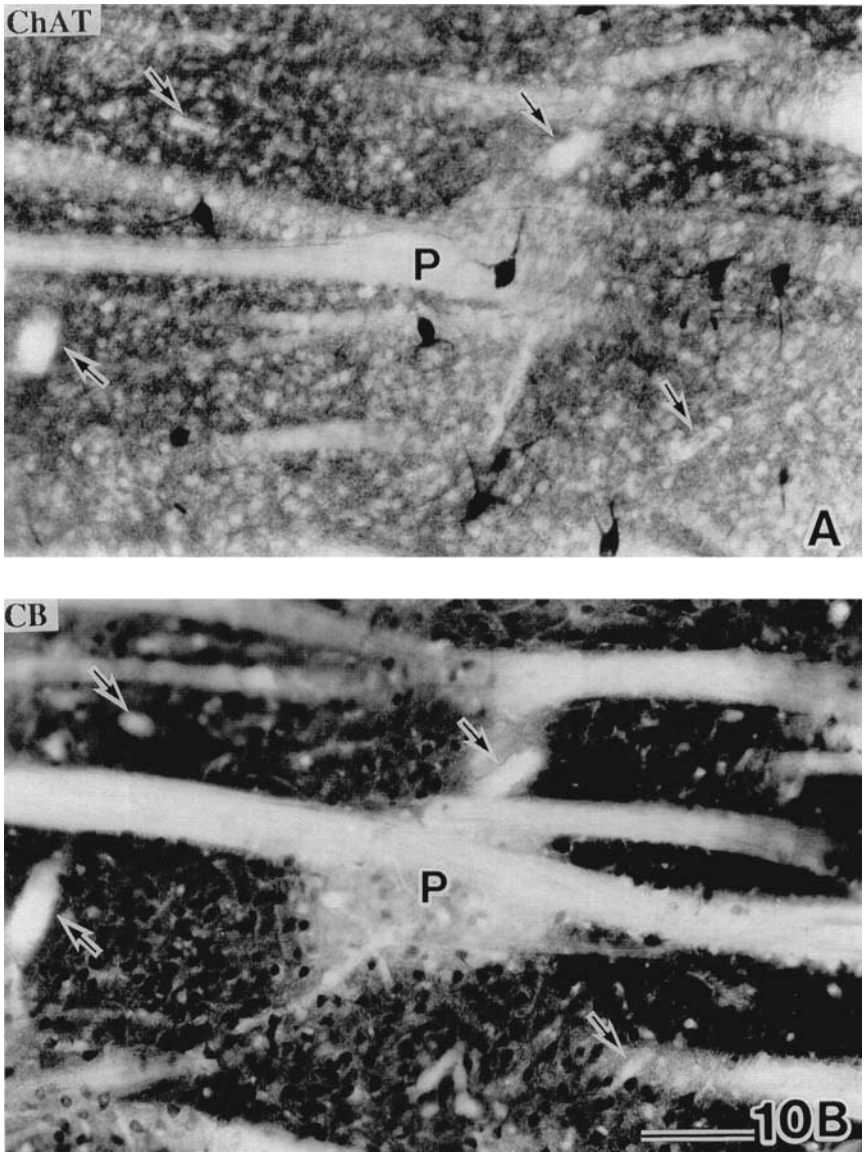

Fig. 10. ChAT-immunoreactive cell in patch compartment (**A**). ChAT-poor area is identical to the calbindin D_{28k} poor patch on the adjacent section (**B**). Arrows indicate capillaries as landmarks. CB, calbindin D_{28k}; P, patch compartment. Scale bar = 100 μm.

striatum respect the compartmental boundaries. Hence the medium spiny cells are not in a position to receive input endings in the two compartments. On the other hand, the dendrites of large sparsely spiny striatal cells do cross the compartmental boundaries (Penny et al., '88; Kawaguchi, '92). These cells are assumed to be cholinergic cells on the basis of morphological similarities to cells immunostained for ChAT. This suggested that some intrinsic striatal cells provide links between the two compartments. In the present study, this has been confirmed for cholinergic, and for parvalbumin- and neuropeptide Y-immunoreactive intrinsic neurons. The axonal ramifications of intrinsic aspiny neurons have not been completely investigated; so it is unclear whether they, like the dendrites of a number of the cells shown here, extend into both patch and matrix compartments.

Possible implication of uneven distribution of structures in the striatum

ChAT poor-immunoreactive regions are seen in the area close to the lateral ventricle and globus pallidus of the striatum. These coincided with calbindin D_{28k} poor patches but they are not found in other calbindin D_{28k} poor regions. In the monkey striatum, ChAT poor-immunoreactive regions have also been identified (Graybiel et al., '86). They form a component of the striosomes, which correspond to the patch compartments of the rat neostriatum.

A gradient of ChAT immunoreactivity is observed in the rat neostriatum, such that a higher density of fibers is found in the dorsolateral part and lower in the ventromedial part. Similar heterogeneity was found by Phelps et al. ('85). This distribution pattern is very similar to that of

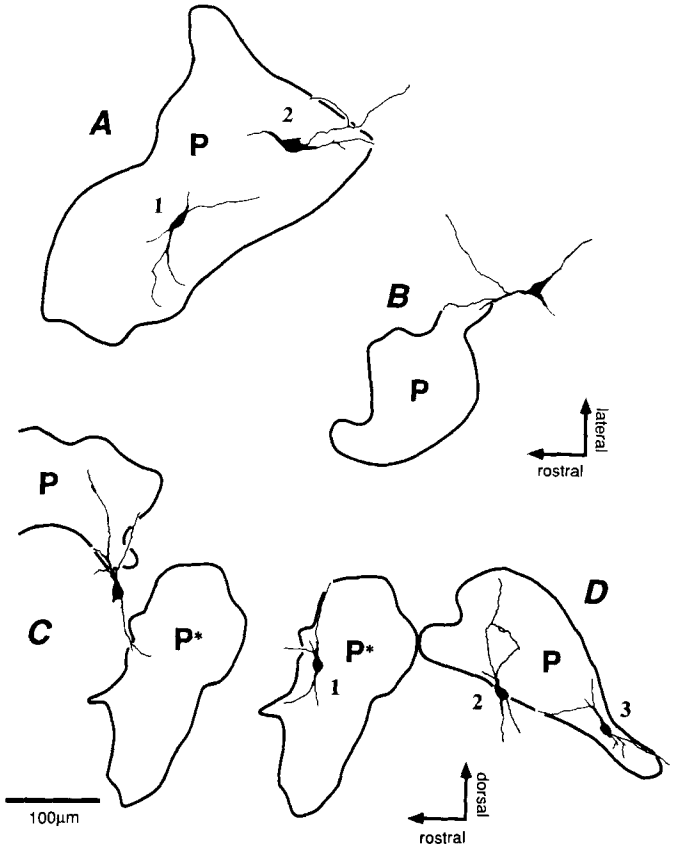

Fig. 11. **A–D:** Reconstruction of 7 neuropeptide Y-immunoreactive cells showing the relationship of dendritic branching patterns to the patch (P) and matrix compartments (external to P). The patch compartments (P*) in C and D are the same patch. A, C and D are sagittal views and B is an oblique horizontal view. Some cells are located in the patch compartment. Their dendrites elongate in the patch, but some of the branches enter the matrix compartment (Cells 2 in A, 1 and 3 in D). The dendrites of the cell in B observe the compartmental boundary. The dendrites of the cell in C elongate into the two patch compartments. The dendrites of the cell on the compartmental boundary elongate into both patch and matrix compartments (cell 2 in D).

dopamine D_2 receptors in the striatum (for a review, see Stoof et al., '92). A quantitative autoradiographic study of dopamine D_2 receptor distribution in the striatum also showed a gradient with a more than twofold greater density laterally than medially (Joyce and Marshall, '87). This study also showed that the region of lower density of dopamine D_2 receptor binding coincided with a region containing a lower density of acetylcholinesterase-stained neurons.

The dorsolateral region of the striatum, which shows higher ChAT immunoreactivity and higher dopamine D_2 receptor binding, is known to receive corticostriatal connections preferentially from the motor cortex (Donoghue and Herkenham, '86; MacGeorge and Faull, '89; Gerfen, '92). This suggests that dopamine-acetylcholine interactions through D_2 receptors may occur more commonly in the motor-related part of the striatum than in other parts.

The corticostriatal pathway utilizes glutamate as its neurotransmitter (Walaas, '81). Large, sparsely spiny, striatal cells show non-*N*-methyl-D-aspartate (NMDA) mediated responses to synaptic stimulation (Kawaguchi, '92) and NMDA receptor stimulation evokes the release of acetylcholine in striatal slices (Lehmann and Scatton, '82). This release is inhibited by dopamine D_2 receptor agonists (Drukarch et al., '90). Striatal cholinergic neurons receive dopaminergic synaptic inputs (Kubota et al., '87; Chang, '88) and show dopamine D_2 receptor gene expression (Le Moine et al., '90). These results may indicate that excitatory inputs from cortex and/or thalamus (Lapper and Bolam, '92) activate large striatal cholinergic neurons via NMDA receptors and this excitation may be inhibited by mesostriatal dopaminergic cells via dopamine D_2 receptors.

Distribution pattern of neuropeptide Y-immunoreactive cells and the coexistence with calbindin D_{28k}

The present results show that some calbindin D_{28k}-immunoreactive neurons in the striatum contain neuropeptide Y immunoreactivity. Neuropeptide Y-immunoreactive cells have previously been identified as medium aspiny intrinsic neurons (Vincent et al., '83). These neurons also contain somatostatin and nitric oxide synthase (NADPH-diaphorase) (Vincent et al., '83; Dawson et al., '91). Our present data indicate that neuropeptide Y-immunoreactive cells are distributed evenly throughout the striatum. Recent studies indicate that nitric oxide is involved in the regulation of blood flow, synaptic efficacy, and glutamate see toxicity (for review, see Bredt and Snyder, '92). Since the neuropeptide Y-positive cells are the sole striatal sub-

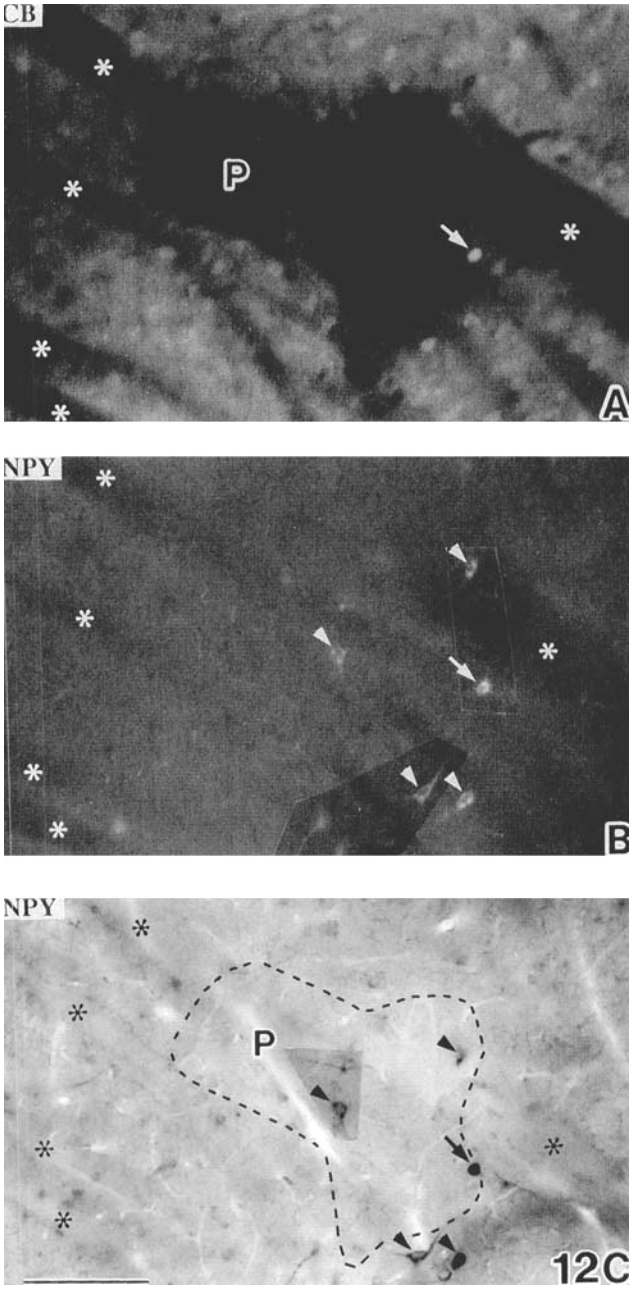

Fig. 12. Neuropeptide Y-immunoreactive neurons in relation to the patch and matrix compartments. **A–C:** The same sagittal section stained by double indirect immunofluorescence with TRITC for calbindin D_{28k} (A), AMCA for neuropeptide Y (B) and subsequently stained by the ABC method with DAB for neuropeptide Y (C). The patch compartments (P) are identified from calbindin D_{28k} poor immunoreactivity in A. These calbindin D_{28k} poor patches are superimposed on the DAB-stained section (broken lines in C). Neuropeptide Y-immunoreactive cells are seen in patch and matrix compartments (arrow and arrowheads in B and C). One cell on the border of compartment contains both neuropeptide Y and calbindin D_{28k} (arrow in A, B and C). Asterisks indicate fiber bundles as landmarks. CB, calbindin D_{28k}; NPY, neuropeptide Y. Scale bar = 100 μm.

population to contain nitric oxide synthase and are uniformly distributed, they may be involved in those functions in the striatum.

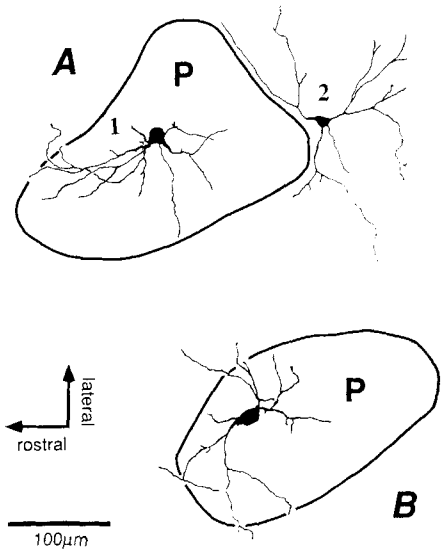

Fig. 13. Reconstruction of 3 parvalbumin-immunoreactive cells showing relationships of the dendritic branching pattern to the patch (P) and matrix compartments (external of P) on the oblique horizontal section. Cell 1 in **A** and the cell in **B** are located in the patch compartment. The dendrites elongate into the patch compartments, but the distal parts of branches enter the matrix compartment. Cell 2 in A localizes just outside the patch and some dendrites observe the compartmental boundary.

Distribution pattern of parvalbumin-immunoreactive structures

The parvalbumin-immunoreactive neuropil of the striatum shows an unequal distribution pattern. It is higher in the lateral and caudal parts of the striatum and lower in the medial part and in a band along the globus pallidus. Larger parvalbumin-immunoreactive cells show a similar distribution pattern. The lateral and caudal parts of the striatum contain many larger cells, whereas the medial part and the band along the globus pallidus contain few larger cells. Since these larger cells tend to have more dendrites than smaller ones, they make for a dense neuropil. The topographical gradient of the density of parvalbumin-immunoreactive neuropil may be related to the heterogeneous distribution of larger parvalbumin-immunoreactive cells in the striatum, i.e., more dendrites of the larger cells make for a denser parvalbumin-immunoreactive neuropil in lateral and caudal parts. This topographical heterogeneity of parvalbumin distribution may be related to sensorimotor function because the lateral and caudal parts of the striatum mainly receive afferents from sensorimotor and auditory cortex (MacGeorge and Faull, '89).

Within the more parvalbumin-immunoreactive neuropil, weak immunoreactive islands are identified and they occasionally, but not always, correspond to calbindin D_{28k} weak patches (Cowan et al., '90; Kita et al., '90). Most of the parvalbumin-immunoreactive cells are located in the matrix and their dendrites are mostly limited to the matrix compartment. This means that the immunoreactive cells in the matrix compartment surround the patches with a high concentration of dendrites and the patch compartments consequently contain a weaker parvalbumin neuropil derived from the few parvalbumin-immunoreactive cells in

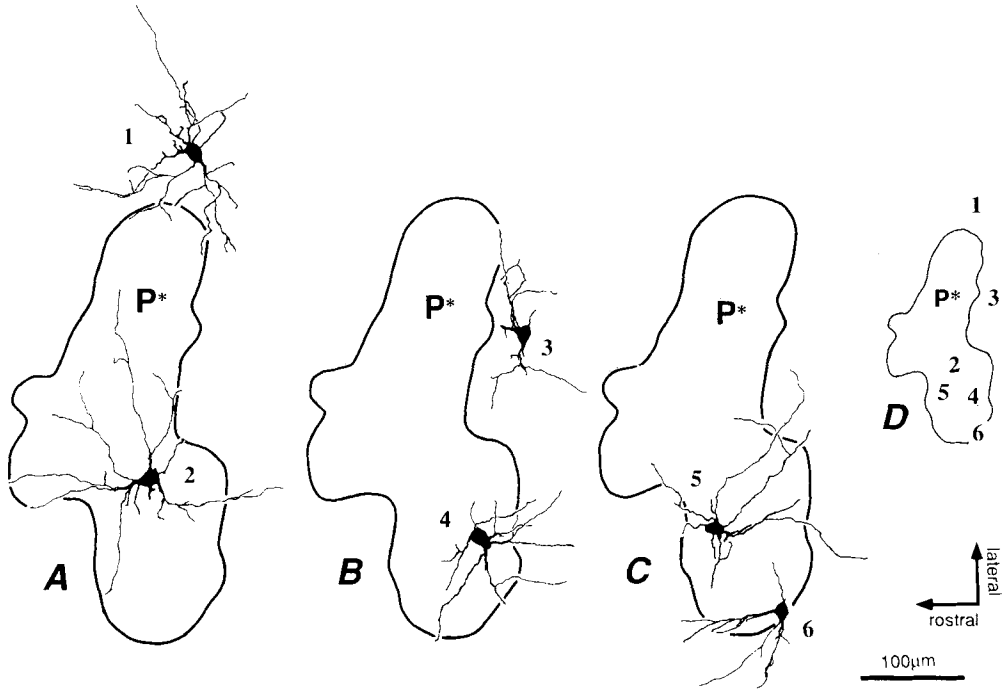

Fig. 14. **A–C:** Reconstruction of 6 parvalbumin-immunoreactive cells showing relationship of the dendritic branching pattern to the patch (P) and matrix compartments (outside area of P) on the oblique horizontal section. The patch compartments (P*) in A–D are the same compartment. The dendrites of cells in the matrix compartment elongate into the matrix, and the distal part of some branches observe the compartmental boundary (cells 1 and 3). Cells in the patch compartment elongate their dendrites into the patch, but some of the distal parts enter the matrix (cells 2, 4, 5). Cell on the boundary (cell 6) elongate the dendrites on patch side into the patch compartment and on matrix side into the matrix compartment. Certain branches of the dendrites in the patch cross the boundary to the matrix compartment. **D** is the illustration showing locations of the cells (1–6) in the *patch* compartment. Note that the cells 2 and 4–6 make a cluster and the dendrites intermingled in the patch compartment.

the patch compartments and from dendrites of cells at the border with the matrix. The variable density of parvalbumin immunoreactivity in certain patches may result from differences in the density of parvalbumin cells and dendrites in the patches and account for the only partial correlation between parvalbumin poor regions and calbindin D_{28k} poor patches seen in the rat neostriatum.

Cell type of ChAT, neuropeptide Y and parvalbumin-immunoreactive neurons

The features of the striatal ChAT-, neuropeptide Y- and parvalbumin-immunoreactive cells found in the present study correspond well to those found in previous studies (Vincent et al., '83; Bolam et al., '84b; Phelps et al., '85; Kubota et al., '87; Celio, '90; Cowan et al., '90; Kita et al., '90).

ChAT-immunoreactive neurons in the rat striatum have large polygonal or fusiform perikarya and two to six primary dendrites with infrequent branchings and no spines. The morphological features of the ChAT-immunoreactive cells observed in this study are similar to type I large neurons (Chang et al., '82), to acetylcholinesterase-positive, Golgi-impregnated type 1 neurons (Bolam et al., '84a) and to giant aspiny neurons (Takagi et al., '84) described by others.

Neuropeptide Y-immunoreactive neurons have medium-sized polygonal or fusiform perikarya and two to five primary dendrites without spines. These features resemble those of type IV medium cells (Dimova et al., '80), and type 2 acetyl cholinesterase-positive, Golgi-impregnated neurons (Bolam et al., '84a) and spindle-shaped, MA1 neurons (Takagi et al., '84) described previously.

Parvalbumin-immunoreactive cells in the present study have medium to large polygonal, fusiform, or round somata with numerous (3–10) radiating primary dendrites with irregular curves, frequent branchings, and no spines. They are quite similar to the type II large and type II medium neurons (Chang et al., '82), type 3 acetyl cholinesterase-positive, Golgi-impregnated neurons (Bolam et al., '84a) and round, MA2 neurons (Takagi et al., '84) described previously.

In the ChAT- or neuropeptide Y-immunoreactive cells, peripheral portions of the dendrites frequently passed out of the plane of section. Biocytin or horseradish peroxidase (HRP) injection studies of striatal large aspiny cells, which were assumed to be cholinergic cells, indicated that the dendritic field was over 500 μm in diameter (Penny et al., '88; Wilson et al., '90; Kawaguchi, '92). The thinness (50 μm) of the sections in the present study, therefore, probably preserved only the central portion of a larger dendritic territory. Neuropeptide Y-positive cells may also have larger dendritic fields and may have lost peripheral parts of the dendrites in our preparations for the same reason. Parvalbumin-immunoreactive neurons showed more complete dendritic fields than the other two type of intrinsic cells. Presumably this was due to the smaller dendritic territory of this cell type. Regardless of these considerations, however, the present results indicate that aspiny

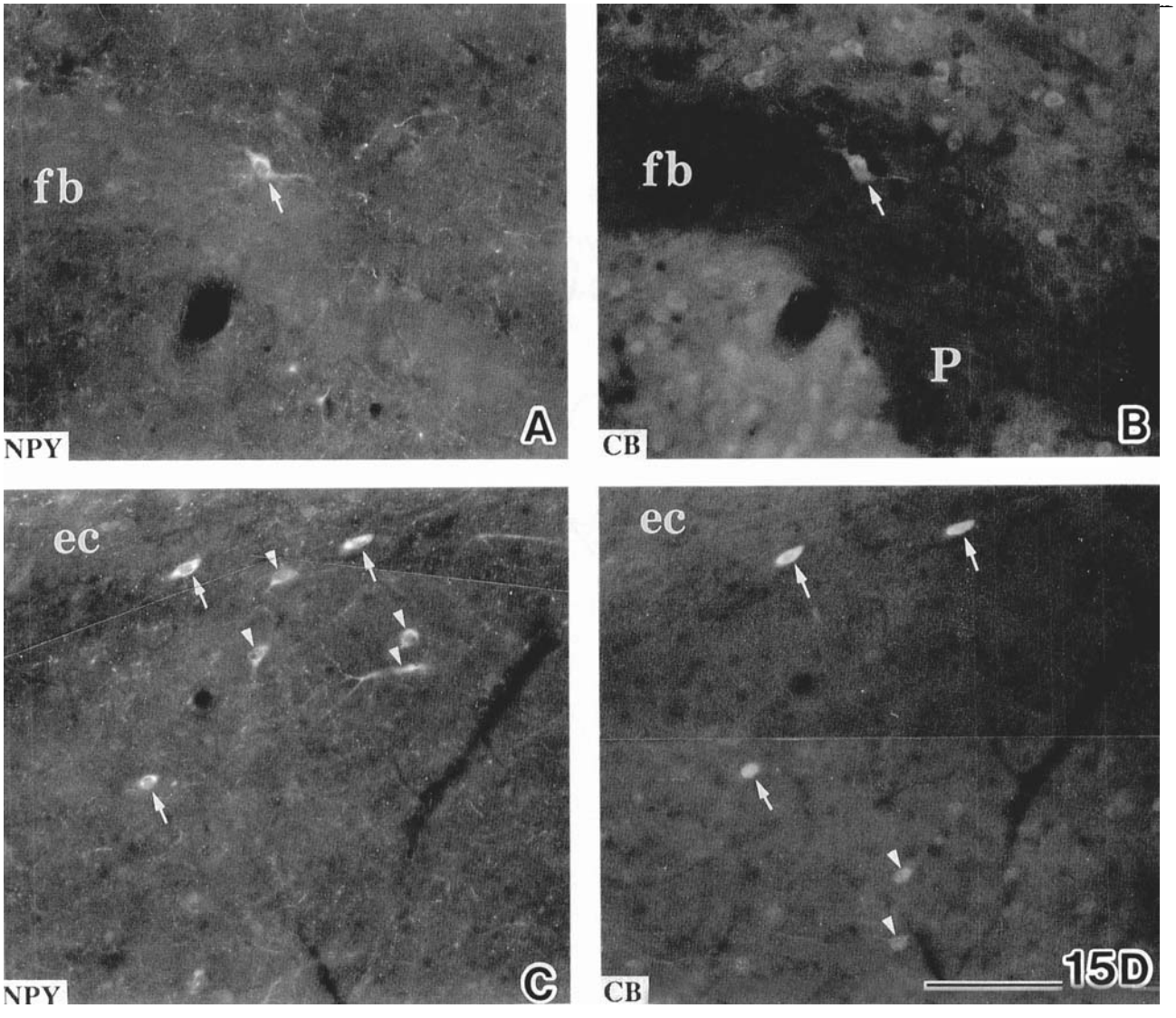

Fig. 15. Coexistence of neuropeptide Y and calbindin D_{28k} in a striatal patch (**A,B**) and in the dorsolateral part of the striatum (**C, D**). A and B: The same section stained by double indirect immunofluorescence with AMCA for neuropeptide Y (A) and TRITC for calbindin D_{28k} (B). A double labeled cell is seen in the patch compartment (arrow). C and D: The same section stained by double indirect immunofluorescence with AMCA for neuropeptide Y (C) and TRITC for calbindin D_{28k} (D). The double labeled cells (arrows) are seen in the dorsolateral part of the striatum, where calbindin D_{28k} immunoreactivity is poor. Some cells show single staining with either neuropeptide Y or calbindin D_{28k} (arrowheads). CB, calbindin D_{28k}; NPY, neuropeptide Y; fb, fiber bundle; ec, external capsule. Scale bar = 100 μm.

intrinsic neurons situated in and adjacent to the patches send dendrites into both patch and matrix compartments. These cells may therefore serve as a means of communication between the two compartments.

ACKNOWLEDGMENTS

This work was supported by a grant from the HFSP "The biology of information processing in the striatum," Special Researchers' Basic Science Program and the Frontier Research Program, RIKEN. The authors greatly appreciate Prof. E.G. Jones for his continuing support and helpful advice, Dr. T. Hashikawa for critical reading of this manuscript, and Miss K. Matsushita for technical assistance. We thank Dr. P.C. Emson for the gift of antiserum to parvalbumin.

LITERATURE CITED

Beckstead, R.M., V.B. Domestick, and W.J.H. Nauta (1979) Efferent connections of the substantia nigra and ventral tegmental area in the rat. Brain Res. *175:*191–217.

Bolam, J.P., B.H. Wainer, and A.D. Smith (1984a) The section-Golgi-impregnation procedure-3. Combination of Golgi-impregnation with enzyme histochemistry and electron microscopy to characterize acetylcholinesterase-containing neurons in the rat neostriatum. Neuroscience *12:*687–709.

Bolam, J.P., B.H. Wainer, and A.D. Smith (1984b) Characterization of cholinenergic neurons in the rat neostriatum. A combination of choline

acetyltransferase immunocytochemistry, Golgi-impregnation and electron microscopy. Neuroscience *12:*711–718.

Bredt, D.S., and S.H. Snyder (1992) Nitric oxide, a novel neuronal messenger. Neuron *8:*3–11.

Celio, M.R. (1990) Calbindin D-28k and parvalbumin in the rat nervous system. Neuroscience *35:*375–475.

Chang, H.T. (1988) Dopamine-acetylcholine interaction in the rat striatum: A dual-labelling immunocytochemical study. Brain Res. Bull. *21:*295–304.

Chang, H.T., C.J. Wilson, and S.T. Kitai (1982) A Golgi study of rat neostriatal neurons: Light microscopic analysis. J. Comp. Neurol. *208:* 107–126.

Chesselet, M.F., and A.M. Graybiel (1986) Striatal neurons expressing somatostatin-like immunoreactivity: Evidence for a peptidergic interneuronal system in the cat. Neuroscience *17:*547–571.

Cowan, R.L., C.J. Wilson, P.C. Emson, and C.W. Heizmann (1990) Parvalbumin-containing GABAergic interneurons in the rat neostriatum. J. Comp. Neurol. *302:*197–205.

Dawson, T.M., D.S. Bredt, M. Fotuhi, P.M. Hwang, and S.H. Snyder (1991) Nitric oxide synthase and neuronal NADPH diaphorase are identical in brain and peripheral tissues. Proc. Natl acad. Sci. USA *88:*7797–7801.

Dimova, R., J. Vuillet, and R. Seite (1980) Study of the rat neostriatum using a combined Golgi-electron microscope technique and serial sections. Neuroscience *5:*1581–1596.

Donoghue, J.P., and M. Herkenham (1986) Neostriatal projections from individual cortical fields conform to histochemically distinct striatal compartment in the rat. Brain Res. *365:*397–403.

Drukarch, B., E. Schepens, and J.C. Stoof (1990) Muscarinic receptor activation attenuates D2 dopamine receptor mediated inhibition of acetylcholine release in rat striatum: Indications for a common signal transduction pathway. Neuroscience *37:*1–9.

Gerfen, C.R. (1984) The neostriatal mosaic: Compartmentalization of corticostriatal input and striatonigral output systems. Nature *311:*461–464.

Gerfen, C.R. (1985a) The neostriatal mosaic: Compartmental distribution of calcium-binding protein and parvalbumin in the basal ganglia of the rat and monkey. Proc. Natl. Acad. Sci. USA *82:*8780–8784.

Gerfen, C.R. (1985b) The neostriatal mosaic. I. Compartmental organization of projections from the striatum to the substantia nigra in the rat. J. Comp. Neurol. *236:*454–476.

Gerfen, C.R. (1987a) The neostriatal mosaic: II. Patch- and matrix-directed mesostriatal dopaminergic and non-dopaminergic systems. J. Neurosci. *7:*3915–3934.

Gerfen, C.R. (1987b) The neostriatal mosaic: III. Biochemical and developmental dissociation of patch-matrix mesostriatal systems. J. Neurosci. *7:*3935–3944.

Gerfen, C.R. (1989) The neostriatal mosaic: Striatal patch-matrix organization is related to cortical lamination. Science *246:*385–388.

Gerfen, C.R. (1992) The neostriatal mosaic: Multiple levels of compartmental organization. Trends Neurosci. *15:*133–138.

Graveland, G.A., and M. DiFiglia (1985) The frequency and distribution of medium-sized neurons with indented nuclei in the primate and rodent neostriatum. Brain Res. *327:*307–311.

Graybiel, A.M. (1990) Neurotransmitter and neuromodulator in the basal ganglia. Trends Neurosci. *13:*243–254.

Graybiel, A.M., R.W. Baughman, and F. Eckenstein (1986) Cholinergic neuropil of the striatum observes striosomal boundaris. Nature *323:*625–627.

Graybiel, A.M., C.W. Ragsdale, E.S. Yoneoka, and R.P. Elde (1981) An immunohistochemical study of enkephalins and other neuropeptides in the striatum of the cat with evidence that the opiate peptides are arranged to form mosaic patterns in register with the striosomal compartments visible by acetylcholinesterase staining. Neuroscience *6:*377–397.

Hendry, S.H.C., E.G. Jones, P.C. Emson, D.E.M. Lawson, C.W. Heizmann, and P. Streit (1989) Two classes of cortical GABA neurons defined by differential calcium binding protein immunoreactivities. Exp. Brain Res. *76:*467–472.

Herkenham, M., and C.B. Pert (1981) Mosaic dostribution of opiate receptors, parafascicular projections and acetylcholinesterase in rat striatum. Nature *291:*415–418.

Johnston, J.G., C.R. Gerfen, S.N. Haber, and D. van der Kooy (1990) Mechanisms of striatal formation: Conservation of mammalian compartmentalization. Dev. Brain Res. *57:*93–102.

Joyce, J.N., and J.F. Marshall (1987) Quantitative autoradiography of dopamine D_2 sites in rat caudate-putamen: Localization to intrinsic neurons and not to neocortical afferents. Neuroscience *20:*773–795.

Kawaguchi, Y. (1992) Large aspiny cells in the matrix of the rat neostriatum In Vitro: Physiological identification, relation to the compartments and excitatory postsynaptic currents. J. Neurophysiol. *67:*1669–1682.

Kawaguchi, Y., C.J. Wilson, and P.C. Emson (1989) Intracellular recording of identified patch and matrix neostriatal neurons in a slice preparation preserving cortical inputs. J. Neurophysiol. *62:*1052–1067.

Kita, H., and S.T. Kitai (1990) Amygdaloid projections to the frontal cortex and the striatum in the rat. J. Comp. Neurol. *298:*40–49.

Kita, H., and S.T. Kitai (1988) Glutamate decarboxylase immunoreactive neurons in rat neostriatum: Their morphological types and populations. Brain Res. *447:*346–352.

Kita, H., T. Kosaka, and C.W. Heizmann (1990) Parvalbumin-immunoreactive neurons in the rat neostriatum: A light and electron microscopic study. Brain Res. *536:*1–15.

Kubota, Y., S. Inagaki, S. Shimada, S. Kito, F. Eckenstein, and M. Tohyama (1987) Neostriatal cholinergic neurons receive direct synaptic inputs from dopaminergic axons. Brain Res. *413:*179–184.

Lapper, S.R., and J.P. Bolam (1992) Input from the frontal cortex and the parafascicular nucleus to cholinergic interneurons in the dorsal striatum of the rat. Neuroscience *51:*533–545.

Lehmann, J., and B. Scatton (1982) Characterization of the exitatory amino acid receptor-mediated release of (^3H) acetylcholine from rat striatal slices. Brain Res. *252:*77–89.

Le Moine, C., F. Tison, and B. Bloch (1990) D_2 dopaminergic receptor gene expression by cholinergic neurons in the rat striatum. Neurosci. Lett. *117:*248–252.

MacGeorge, A.J., and R.L.M. Faull (1989) The organization of the projection from the cerebral cortex to the striatum in the rat. Neuroscience *29:*503–537.

Penny, G.R., C.J. Wilson, and S.T. Kitai (1988) Relationship of the axonal and dendritic geometry of spiny projection neurons to the compartmental organization of the neostriatum. J. Comp. Neurol. *269:*275–289.

Phelps, P.E., C.R. Houser, and J.E. Vaughn (1985) Immunocytochemical localization of choline acetyltransferase within the rat neostriatum: A correlated light and electron microscopic study of cholinergic neurons and synapses. J. Comp. Neurol. *238:*286–307.

Stoof, J.C., B. Drukarch, P. de Boer, B.H.C. Westerink, and H.J. Groenewegen (1992) Regulation of the activity of striatal cholinergic neurons by dopamine. Neuroscience *47:*755–770.

Takagi, H., P. Somogyi, and A.D. Smith (1984) Aspiny neurons and their local axons in the neostriatum of the rat: A correlated light and electron microscopic study of Golgi-impregnated material. J. Neurocytol. *13:*239–265.

Vincent, S.R., O. Johansson, T. Hökfelt, L. Skirboll, R.P. Elde, L. Terenius, J. Kimmel, and M. Goldstein (1983) NADPH-diaphorase: A selective histochemical marker for striatal neurons containing both somatostatin- and avian pancreatic polypeptide (APP)-like immunoreactivities. J. Comp. Neurol. *217:*252–263.

Walaas, I. (1981) Biochemical evidence for overlapping neocortical and allocortical glutamete projections to the nucleus accumbens and rostral caudateputamen in the rat brain. Neuroscience *6:*399–405.

Wilson, C.J., H.T. Chang, and S.T. Kitai (1990) Firing patterns and synaptic potentials of identified giant aspiny interneurons in the rat neostriatum. J. Neurosci. *10:*508–519.